THE PENNSYLVANIA STATE UNIVERSITY
SCHREYER HONORS COLLEGE

DEPARTMENT OF MECHANICAL AND NUCLEAR ENGINEERING

DESIGN OF A REGENERATIVE NOZZLE FOR ALUMINUM-WATER COMBUSTION

KEVIN CIASULLO
SPRING 2016

A thesis
submitted in partial fulfillment
of the requirements
for a baccalaureate degree
in Mechanical Engineering
with honors in Mechanical Engineering

Reviewed and approved* by the following:

Thomas Cawley
Research Associate
Thesis Supervisor

Zoubeida Ounaies
Professor of Mechanical Engineering
Honors Adviser

* Signatures are on file in the Schreyer Honors College.

ABSTRACT

This work details the design of a new converging regenerative nozzle for an aluminum-water combustor. The combustion reaction involves an intimate mixing of aluminum powder and steam with liquid water used as a periphery wall coolant. The nozzle provides two necessary functions for this system: to create backpressure within the research combustor and to generate steam to be transported upstream and mixed with the aluminum powder.

The nozzle design features a single pass circular channel that spirals around the converging wall. Three models have been developed in order to determine the conditions in the channel. The first is a simple combustion model to determine the potential energy transfer into the nozzle based on the inlet and exit conditions of a steady state reaction. The second model uses a chemical equilibrium analysis in order to calculate the convection and radiation heat transfer into the nozzle from the combustion reaction. The third model calculates the pressure drop through the channel. Future work should check the validity of these models and incorporate more efficient heat transfer methods.

TABLE OF CONTENTS

LIST OF FIGURES

LIST OF TABLES

Nomenclature

A_c	Cross sectional area
A_f	Liquid cross sectional area
A_g	Gas cross sectional area
$A_{s,n}$	Surface area of the nozzle combustor side
Bo	Boiling number
C_f	Confinement number
Co	Convection number
C_{pf}	Liquid heat capacity at a constant pressure
D	Diameter
D_h	Hydraulic Diameter
F	Reynolds number factor
f_f	Liquid wall friction
f_g	Gas wall friction
$f_{2\emptyset}$	Two-Phase friction factor
g	gravitational acceleration
G	mass flux
G_w	Mass flux at the wall
h	Heat transfer coefficient
h(z)	enthalpy at position z
h_{fg}	enthalpy of vaporization
h_{nb}	Nucleate boiling heat transfer coefficient
h_{sp}	Single phase heat transfer coefficient
h_{tb}	Turbulent two-phase heat transfer coefficient
ΔH	Enthalpy of Combustion
ΔH_R^o	Enthalpy of Reaction at standard conditions
ΔH_s	Sensible Enthalpy change from standard conditions (298 K)
k	Thermal conductivity
k_f	Liquid thermal conductivity

L	Pipe length
$\dot{m}$	mass flow
$\dot{m}_f$	Liquid mass flux
$\dot{m}_g$	Gas mass flow
Nu_D	Nusselt number based on Diameter
Pr	Pradtl number
Pr_f	Liquid Pradtl Number
ΔP	Pressure drop
ΔP_{sat}	Difference between local wall pressure and saturation pressure
q	Heat
q_{conv}	Convective heat transfer
q_{rad}	Radiative Heat transfer
q_w”	Wall heat flux
Re_D	Reynolds number based on diameter
Re_f	Liquid Reynolds number
Re_f	Liquid Reynolds number
Re_g	Gas Reynolds number
S	Suppression Factor
T_∞	Free stream temperature
T_w	Wall temperature
ΔT_{sat}	Difference between local wall temperature and saturation temperature
u	Horizontal velocity
u_e	Horizontal exhaust velocity
u_f	Liquid horizontal velocity
u_g	Gas horizontal velocity
$\bar{u}$	Bulk fluid horizontal velocity
v_f	Liquid specific volume
v_{fg}	specific volume difference between gas and liquid phase
v_g	Gas specific volume
x	vapor quality

X_{tt}	Martinelli parameter
z	horizontal distance
μ	Viscosity
μ_f	Liquid viscosity
μ_g	Gas viscosity
ρ	Density
ρ_f	Liquid density
ρ_g	Gas density
$\bar{\rho}$	Bulk fluid density
σ	Surface tension
σ_B	Stefan-Boltzman's constant

ACKNOWLEDGEMENTS

There are several people I would like to thank for their help with this thesis. Firstly, I would like to thank my mother and my father for all of their love and support. They have always been there for me. I would also like to thank my supervisor Tom Cawley for his guidance and support throughout this project. Finally, I thank my friends for always being there to get me through the tough times.

Chapter 1

Introduction

1.1 Background

Many researchers are interested in the subject of aluminum combustion because of its many practical qualities as a potential power source. One reason aluminum combustion is sought after is the fact that aluminum has a very high energy density. Data from Kulakov [1] and Domalski [2] are plotted in Figure 1. Aluminum dwarfs the other substances with an energy of 84 MJ/L compared to gasoline (34 MJ/L), kerosene (33 MJ/L), and natural gas (9 MJ/L). This quality is very useful where storage is limited because the same amount of storage can produce a much higher energy output.

Another quality of aluminum is that it is relatively lightweight. Aluminum has a density of 2700 kg/m^3 while steel and nickel are 7850 kg/m^3 and 8900 kg/m^3, respectively. When comparing the specific energy of metal fuels in Figure 1, aluminum (31 MJ/kg) falls behind Lithium (43MJ/kg) but is significantly higher than magnesium (25 MJ/kg). The low density can keep the mass of the fuel lower while maintain the same volume of fuel.

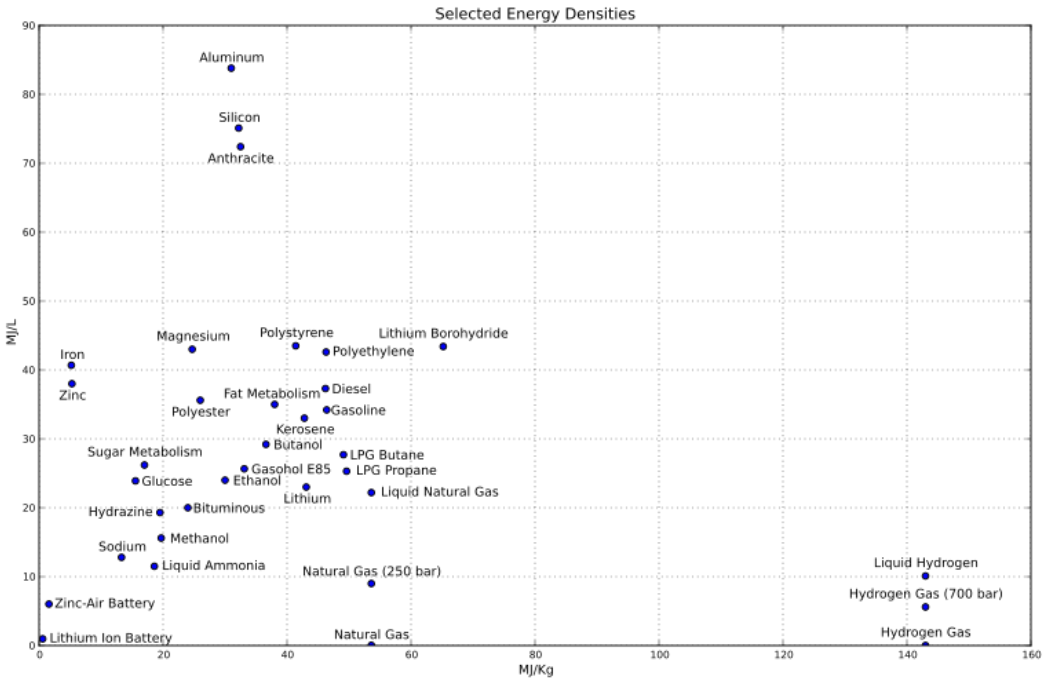

Figure 1: Energy density and specific energy of selected materials by Scott Dial [3]

Aluminum is also very safe. Gasoline and hydrogen are highly flammable and while that is useful in a combustion engine, it is a serious safety hazard while being stored. Hydrogen also has the issue with needing to be pressurized, increasing its safety risk. Aluminum does not have these issues because it forms a very thin oxide layer. This layer is very tough and highly resistant to weathering. Unlike when steel oxidizes, aluminum oxide, commonly called alumina, does not flake and disintegrate which allows the aluminum to remain stable and usable for long periods.

While the potential energy benefits of aluminum combustion are great, there are several technical difficulties. First, the inner aluminum must be exposed. This is not a trivial matter because of the initial temperature requirements. Merzhanov, et al [4] suggested that the ignition temperature of aluminum particles would occur at the melting point of the alumina shell, 2300 K. Ermakov, et al [5] observed ignition temperatures of ~2000-2100 K and concluded that the oxide

layer's integrity failed. Lokenbakh, et al [6] used varying heating and ambient conditions and observed temperatures as low as 1000 to 1300 K. This is still a very steep initial requirement.

Aluminum combustion is a very energetic process that can reach flame temperatures of up to 4000 K [7]. The flame is well above the melting temperatures of almost all materials and the local heat flux can easily compromise the integrity of any exposed part.

Alumina is also hard and is often used as an abrasive. This property makes it very dangerous as it flows from the combustion chamber because of the possible damage.

1.2 Design Needs

The goal for the thesis is to design a small regenerative nozzle subsystem for an aluminum-water combustion system. The specifications and requirements of the system and nozzle are as follows:

- Water is the chosen oxidizer
- The nozzle must supply at least enough oxidant water vapor in order to sustain the combustion
- The oxidizer at the outlet must be at least a saturated vapor
- The oxidizer outlet pressure must exceed the combustion chamber pressure
- The nozzle must attach to the current hardware
- The nozzle must allow for interior combustion temperature measurements
- The integrity of the nozzle must not be comprised
- A heat transfer model must be created

1.3 Literature Review

1.3.1 Rocket Cooling

The conditions inside the combustion chamber consist of extremely high temperatures, high pressures, high heat fluxes, and abrasive flow. Fortunately, research has been conducted on similar conditions inside liquid rocket engines. The solutions often used in rocket applications are injection, ablative, and regenerative cooling. Because of the high heat fluxes involved (~1-100 MW) [8,9], these cooling methods are rarely used alone.

Injection cooling consists of flowing coolant into the combustion chamber or engine in order to coat the engine walls and nozzle with a film. The three main types of injection cooling are transpiration, film, and curtain. The coolant absorbs thermal energy, protecting the walls and nozzle from the exhaust flow. Often the fuel is used as the coolant because it is easier to use over any entirely separate coolant. The fuel is a reasonable coolant because the fuel rich conditions near the wall combust at lower temperatures than stoichiometric conditions. The cooling becomes less effective as the film becomes more stoichiometric however overcooling can be detrimental to the rocket performance. [10]

The three methods of injection cooling are similar but the difference between them lies in the cooling mechanisms:

1. Transpiration cooling uses a porous material on the walls that allows a fluid to seep into the chamber. This provides two principal heat reduction mechanisms. First, the coolant absorbs heat from the porous wall and second it provides the protective film layer as can be seen in Figure 2. Terry and Caras [11] note that transpiration cooling can provide the greatest theoretical cooling effectiveness

compared to other cooling methods but the problem lies with creating a structurally sound material.

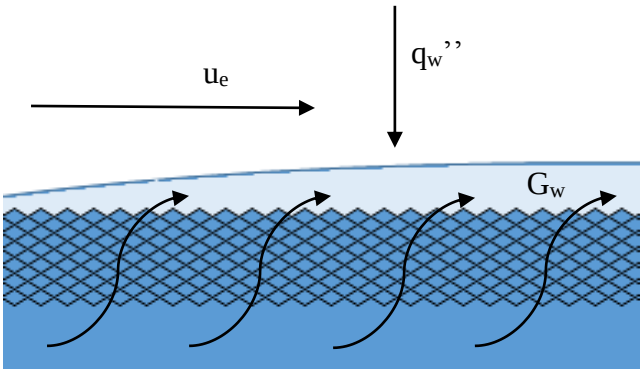

Figure 2: Transpiration cooling

2. Film cooling uses small openings along the wall to flow coolant into the chamber. Figure 3 shows the coolant fluid flow's a thin boundary layer film that protects the wall and lowers the surface temperature. Film cooling has been used in rocket designs since the German V-2 nozzle [11]. It is a very well researched mechanism and is still used today in rockets and high temperature turbine applications.

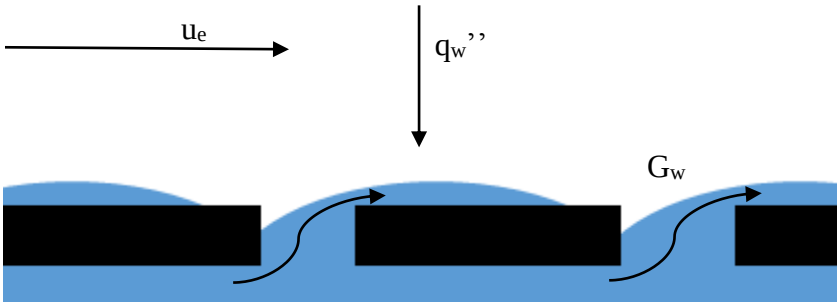

Figure 3: Film cooling

3. Curtain cooling is when the propellant injectors are arranged in such a way as to promote the arrangement of cooler gases at the walls. Figure 4 shows a simplified example.

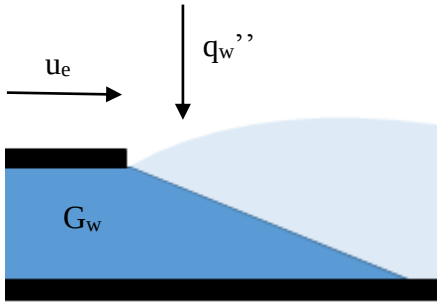

Figure 4: Curtain cooling

Ablative cooling consists of using a sacrificial material to absorb thermal energy. The material is vaporized or eroded away keeping the integrity of the part safe. Most famously ablative cooling was used as a heat shield for the capsules of the Mercury, Gemini, and Apollo spacecraft. While the advantages of ablative cooling include simplicity, reliability and ease of fabrication, the material does erode [12]. Using an ablative material in a rocket engine can maintain the temperatures at safe levels but the geometry of the throat can change which may significantly affect rocket performance.

Regenerative cooling is one of the most commonly used and studied cooling methods in rocket design. The design simplifies to the chamber and nozzle of the rocket have small channels along their outer perimeter. Fuel and/or oxidizer is used as a coolant and is pumped through these channels. The coolant(s) are then pumped into the chamber to be combusted. Regenerative cooling is a balance between the rejected energy of the combustion and the energy absorbed by the coolant [13]. Unlike in injection cooling where there is excess fuel not being combusted, regenerative cooling allows the heat transfer away from the engine to not go to waste. The increase of the initial energy of the reactants enhances the exhaust velocity by 0.1-1.5% [14] but the overall engine performances increases by less than 1% [15].

1.3.2 Two Phase Fluid Dynamics and Heat Transfer

Inside the regenerative nozzle two-phase flow heat transfer occurs. This is a very complex and challenging area of research. Previous studies have been performed with different fluids, mass fluxes, heat fluxes, pressures, and qualities but the results often conflicted.

It is imperative to understand the boiling curve before analyzing two-phase heat transfer. Figure 5 shows the boiling curve for water at a specified pressure is a function of the excess wall temperature. In general, heat flux increases as the wall temperature increases. This is reasonable in a convective heat transfer where the heat flux depends on the heat transfer coefficient and the temperature difference (Eq 1). Boiling however involves two different phases, which affect the convective coefficient and can radically affect heat transfer.

$$q''_{conv}{}' = h * (T_w - T_\infty) \tag{1}$$

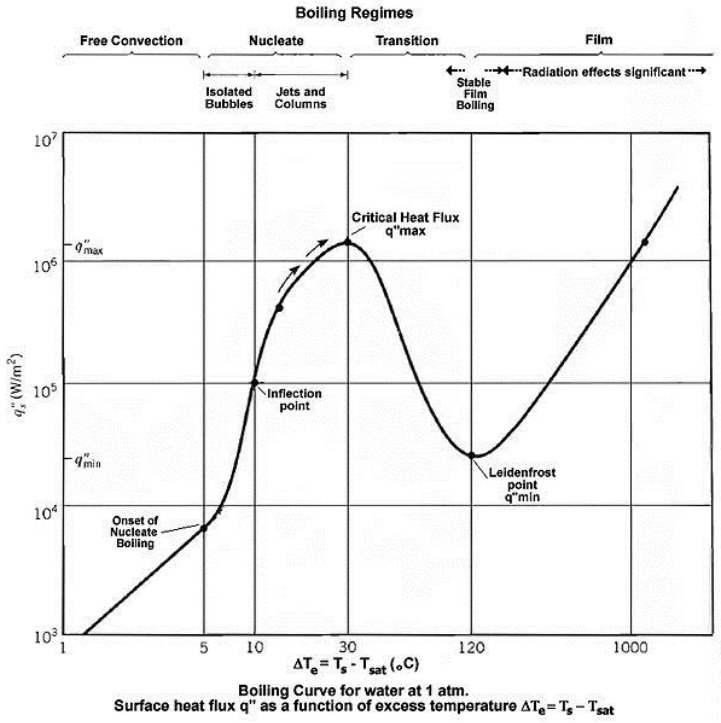

Figure 5: Pool boiling regimes for water at 1 atmosphere by the Pennsylvania State University [16]

When the excess temperature is less than 5 ^{o}C the boiling regime is considered to be free convection. The heat transfer does not produce noticeable bubbles and instead the water becomes a superheated liquid. As can be observed in Figure 5, the heat flux is directly proportional to the excess wall temperature, indicating that the heat transfer coefficient does not change noticeable.

As the excess wall temperature increases nucleate, boiling begins. This initially starts with isolated bubbles then continues onto jets and columns of bubbles. On a horizontal plate the liquid in contact with the wall vaporizes and rises, allowing new liquid to flow in and replace the vaporized fluid. The movement of the fluid increases the heat transfer coefficient and the heat flux rapidly increases. As more bubbles form and rise, the fluid flow becomes more turbulent increasing the heat flux.

Eventually at about 30 ^{o}C excess, the nucleate boiling sites coalesce into a thin film and dry-out occurs. The film is unstable as liquid continually comes into contact with the surface only to be vaporized immediately. This regime is referred to as transitional because it is an unstable combination of nucleate and film boiling. Once the film becomes stable, the regime becomes film boiling. At dry-out the heat flux is at a maximum value known as the Critical Heat Flux (CHF). Once the thin vapor film forms, the wall temperature increases rapidly. This is due to the low heat transfer properties of water vapor. The rapid temperature rise is very problematic as it can quickly compromise the integrity of the vessel walls.

In two-phase tubular flow, liquid and vapor travel together in different flow regimes. The adiabatic regimes are not quantitatively defined well and instead are qualitatively observed, and depend specifically on the flow quality, flow rate, and flow orientation. Table 1 shows the relationship between quality and flow rate and the regimes in a vertical pipe. Figure 6 gives visual representation for the regimes labeled in Table 1.

Table 1: Qualitative classification of two-phase flow regimes

Flow Quality	Flow Rate	Flow Regime
Low	Low and Intermediate	Bubbly
	High	Dispersed Bubbly
Intermediate	Low and Intermediate	Plug/Slug
	High	Churn
High	High	Annular
	High (post dry-out)	Mist

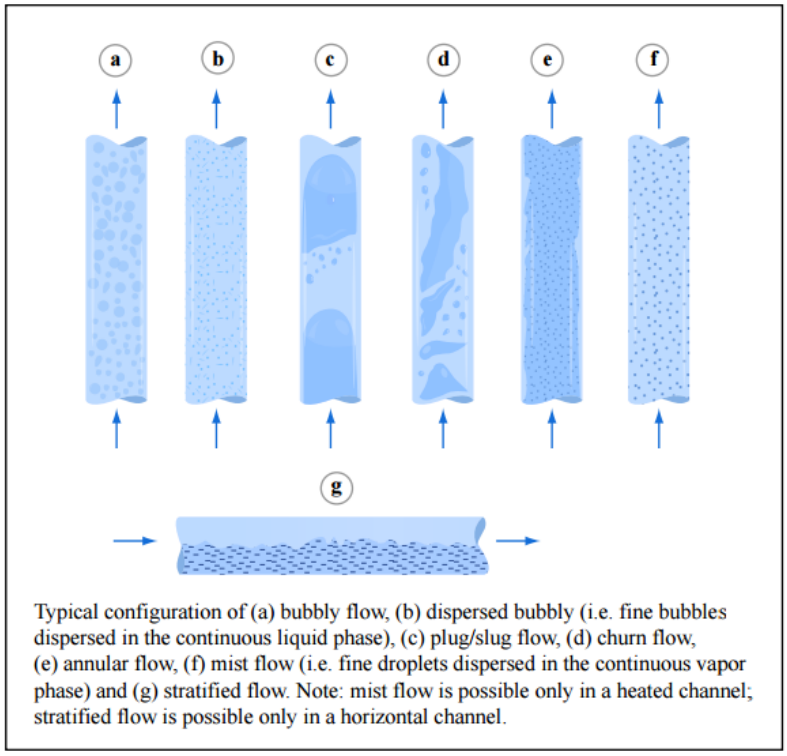

Typical configuration of (a) bubbly flow, (b) dispersed bubbly (i.e. fine bubbles dispersed in the continuous liquid phase), (c) plug/slug flow, (d) churn flow, (e) annular flow, (f) mist flow (i.e. fine droplets dispersed in the continuous vapor phase) and (g) stratified flow. Note: mist flow is possible only in a heated channel; stratified flow is possible only in a horizontal channel.

Figure 6: Visual representation of two-phase flow regimes by MIT OpenCourseWare [17]

The regimes of a vertical and a horizontal tube are similar but the main difference comes from buoyancy effects. The flow tends to be stratified with vapor above the liquid.

Boiling inside tubes follows the same general form as the boiling curve. First, nucleate bubbling begins. The bubbles grow and coalesce into plugs and slugs. Then those coalesce and push the liquid to the sides in annular flow. Eventually dry-out will occur. In vertical flow, the dry-out occurs evenly in the tube while in horizontal flow dry-out occurs on the upper section of tube first because of stratification. Figure 7 gives an example of a conventional vertical boiling tube where the transitions between each regime can be observed.

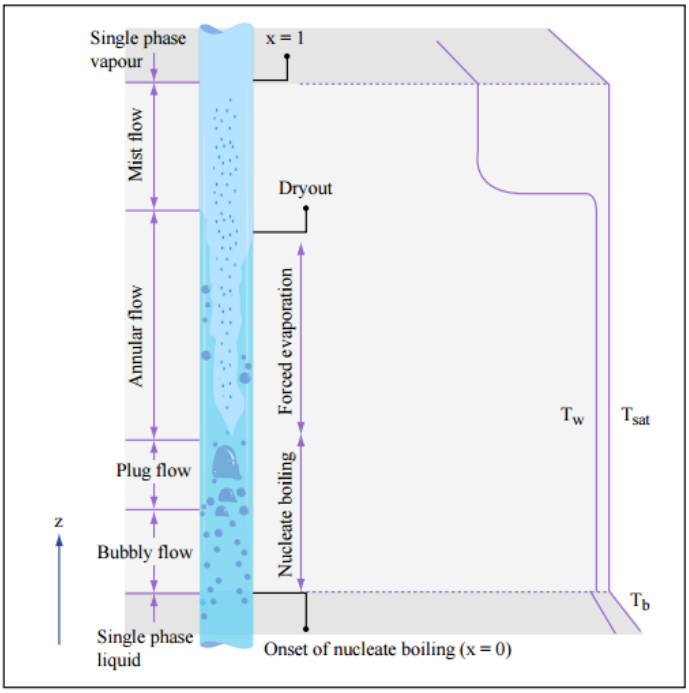

Image by MIT OpenCourseWare.

Figure 7: Flow boiling regimes in a tube by MIT OpenCourseWare [17]

The diameter of the tube does affect the observed regimes slightly. Kandlikar (2002) [18] proposed identifying different sized channels: conventional channels (D_h larger than 3mm), mini-channel (D_h between 200 μm and 3mm), and micro-channel (D_h between 10 and 200 μm) in order to standardize comparisons. Mini-channel boiling regimes are slightly different from their larger counterparts. Conwell and Kew (1992) [19] identified three flow regimes that are

sufficient to describe the patterns they observed. They are isolated bubble flow, confined bubble flow, and annular-slug flow. Because of the confined space, instabilities occur causing local dry-outs on the wall under some conditions. This is especially apparent in multi-channel systems due to pressure drop fluctuations.

Several two-phase flow-boiling models exist in literature. Chen [20] was the first to develop a widely used model. His analysis had the turbulent two-phase heat transfer coefficient (h_{tb}) be made of a single phase convective heat transfer term (h_{sp}) and a nucleate boiling term (h_{nb}) with a Suppression Factor (S) and a Reynolds Number Factor (F). The suppression factor is a function of the Reynolds number (Eq. 6) and the Reynolds number factor is a function of the Martinelli parameter (X_{tt}), see Eq. 3 &4. Gungor and Winterton [21] modified Chen's correlation, specifically observing that the Suppression Factor is also a function of the Reynolds number factor, S = fn(F,Re_f), and the Reynolds number factor is also a function of the Boiling Number (Bo), F = fn(Bo, X_{tt}).

$$h_{tb} = S * h_{nb} + F * h_{sp} \tag{2}$$

Where,

For $1/X_{tt} > 0.1$,
$$F = 2.35(\frac{1}{X_{tt}} + 0.213)^{0.736} \tag{3}$$

For $1/X_{tt} \leq 0.1$,
$$F = 1 \tag{4}$$

$$h_{sp} = 0.023 Re_f^{0.8} Pr_f^{0.4} (\frac{k_f}{D_h}) \tag{5}$$

$$S = 1/(1 + 2.53 * 10^{-6} Re_f^{1.17}) \tag{6}$$

$$h_{nb} = 0.00122 (\frac{k_f^{0.79} c_{pf}^{0.45} \rho_f^{0.49}}{\sigma^{0.5} \mu_f^{0.29} h_{fg}^{0.24} \rho_g^{0.24}}) \Delta T_{sat}^{0.24} \Delta P_{sat}^{0.75} \tag{7}$$

$$X_{tt} = \left(\frac{1-x}{x}\right)^{0.9} \left(\frac{\rho_g}{\rho_f}\right)^{0.5} \left(\frac{\mu_f}{\mu_g}\right)^{0.1} \quad (8)$$

Shah [22] proposed a correlation in graphic form using the Boiling Number (Bo) and the Convection Number. This simplified the components of nucleate boiling and forced convection. The Convection Number (Co) replaced the Martinelli parameter from Chen's correlation because the viscous ratio was found to not have a significant influence. The simplification allows Shah's model to be applied easily however, the accuracy is restricted especially concerning pressure effects [23].

Applying current flow boiling models to mini-channels has led to questionable results. Kew and Cornwell (1997) [24] analyzed accuracy of the established correlations for tubes with diameters of 1.39-3.69 mm. They defined Confinement Number (C_f) in Eq. 9 to account for the fluid flow and diameter. They concluded that the correlations predicted the heat transfer coefficients reasonably well for the largest tubes but performed badly when applied to the smaller tubes where the Confinement Number was in excess of 0.5.

$$C_f = \frac{[\sigma/(g(\rho_f - \rho_g))]^{0.5}}{D_h} \quad (9)$$

Kandlikar [18] concluded that flow-boiling correlations for larger diameter tubes could be applied as a first order estimate to mini and micro-channels. He also stated that more research was needed on the effects of inlet flow conditions and CHF data in single and parallel mini and micro-channels.

Zhang et al. [23] observed that current correlations gave reasonably acceptable predictions for flow boiling in mini-channels in certain flow conditions. Lockhart and Martinelli [25] divided the flow into four conditions:

1. When $Re_f < 1000$ and $Re_g < 1000$ both liquid and gas flows are laminar.
2. When $Re_f > 2000$ and $Re_g < 1000$, the liquid flow is turbulent whereas the gas flow is laminar.
3. When $Re_f < 1000$ and $Re_g > 2000$, the liquid flow is laminar whereas the gas flow is turbulent.
4. When $Re_f > 2000$ and $Re_g > 2000$ both liquid and gas flows are turbulent.

Zhang et al. concluded that the Chen [20], Liu-Winterton [26], and Kandlikar [27] correlations work well for saturated flow boiling but they are not physically sound when the liquid flow is laminar. They also concluded that the generalized Chen Correlation gave physically sound and good predictions for all four flow conditions. Overall there are several correlations that can be applied in different flow conditions but their accuracy is a concern.

Chapter 2

Design

2.1 General Design

Several different designs were considered for the nozzle subsystem. Since this is the first nozzle of its kind, the design is focused on the survivability of the part and gathering useful data. The data collected will provide a better understanding of the internal combustion conditions and the heat transfer model for future designs. The current design features regenerative cooling, additive manufacturing, and a direct connection to the current hardware.

Figure 8 shows a three-dimensional view of the nozzle and Appendix A shows some dimensions of an example nozzle. The fixed design features included a converging nozzle to a throat diameter of 0.594 inches. This was specified because of previous work performed with the same dimension. The overall dimensions of the nozzle are an outside diameter of 3.62 inches and a length of 4.00 inches. The top of the nozzle features a shoulder in order to fit into the liner of the current hardware. The threads also fit into the current hardware and secure the nozzle. The inlet and exit channels feature a flat face on the surface of the nozzle for a fitting to be welded in place. The coolant plumbing will attach to these fittings. The hole on the side of the nozzle allows thermocouple to be implemented into the combustion chamber.

Figure 8: 3D CAD Nozzle Representation

2.2 Cooling Design

The cooling methods chosen for the combustion system are curtain cooling and regenerative cooling. Curtain cooling was applied in previous work done and was found to be effective at keeping wall temperatures within safe limits. A previous project used much of the same hardware so it is relatively easy to reappropriate it and modify specific parameters. Liquid water will be used as the coolant for two reasons. First, water has a high heat of vaporization which allows to provide a superior boundary between the flame and wall. Second, water is the oxidizer used in the combustion.

Regenerative cooling is necessary because of the system requirements and its excellent cooling power. Liquid water will flow into the nozzle channels and vaporize into steam. The steam will then travel into the combustion chamber via injectors at the top. The regenerator is a single, one-pass, counter flow channel. It is designed for simplicity and survivability. The single

channel is circular and maintains a distance of one diameter away from the combustion-side nozzle wall. This is to ensure that the high heat and abrasive alumina do not compromise the channel integrity. The channel spirals around the throat and continues upwards to the top where it returns to the bottom of the nozzle. A cross sectional view in Figure 9 shows the interior channel. Pressure and temperature measurements will be made just before the inlet and after the outlet in order to better understand the heat transfer process.

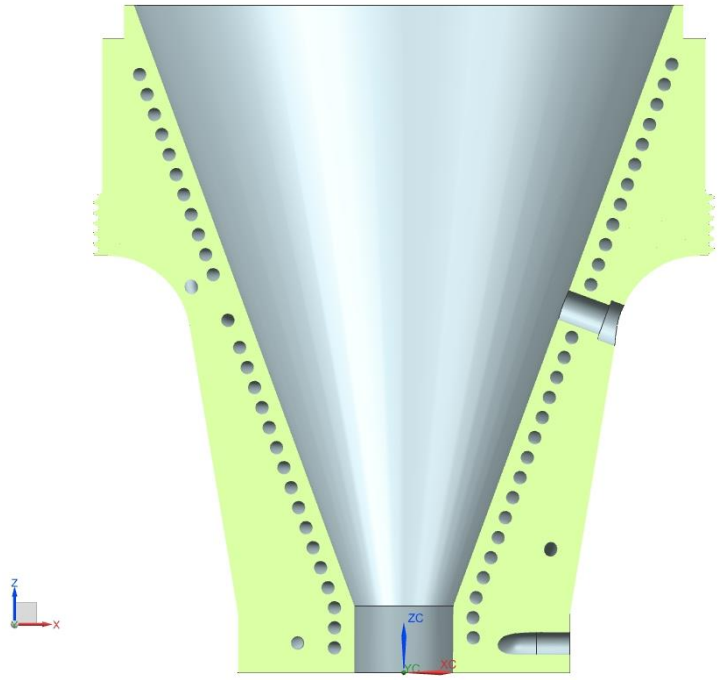

Figure 9: Cross sectional view of the nozzle design

2.3 Manufacturing

The manufacturing process chosen for the nozzle was additive direct metal laser sintering (DMLS). DMLS is a process that divides a computer model into layers. The machines analyzes these layers and physically lays metal powder ~20 microns thick on a platform. A laser sinters a

pattern in the metal bed. The platform descends slightly and another layer of powder is placed upon the sintered one. The next pattern is sintered and the process repeats. The laser can sinter several layers deep, welding one layer onto the previous. The final product is a part made of the layered patterns. DMLS has a high tolerance and allows for complex parts to be created with ease. Several other manufacturing methods were considered but they were found to be less effective.

The chosen metal is Inconel 718. Inconel 718 is a nickel super alloy often used in high temperature applications such as turbine blade. It was chosen for its survivability.

Chapter 3

Projections

3.1 Combustion Model

In order for a heat transfer analysis to be performed on the nozzle, a basic combustion model in the chamber must first be created. Several simplifying assumptions are based on the planned experimentation and are as follows:

1. The only reaction considered is:

$$2\ Al + 3\ H_2O\ \rightarrow Al_2O_3 + 3\ H_2 \quad (9)$$

2. The oxidizer is water vapor
3. The curtain coolant is known as diluent water and enters as a liquid
4. The reaction is initiated by an ignitor and anchored to the point of injection without any consideration for flame speed

The combustion model included variable mass flow rates, initial temperatures, and exit temperatures. An example of the initial conditions can be found in Table 2. The steam entering the chamber is the coolant from the regenerative nozzle. The exit conditions assume a perfect reaction and the products have the same temperature. An example of the exit conditions is found in Table 3. Eq 10 details the heat transfer into the nozzle from the reaction by associating the sensible heats, the heat of the reaction, and the heat of vaporization of the diluent water at steady state conditions. The vaporization of the diluent water must be accounted for in the sensible heats of the products.

Table 2: Combustion reactants initial conditions

	Al	H2O(g)	diluent H2O(L)
mass flow(lb/s)	0.001	0.00115	0.003
mass flow(g/s)	0.4536	0.522	1.361
Temperature (K)	300	700	300

Table 3: Combustion products exit conditions

	Al2O3	H2O(g)	H2
mass flow(lb/s)	0.00189	0.00315	0.00011
mass flow(g/s)	0.86	1.42884	0.0504
Temperature (K)	1200	1200	1200

$$q_w = \sum \Delta H_{s,reac} + \Delta H_R^o - \sum \Delta H_{s.prod} \quad (10)$$

Where

q_w = Nozzle wall heat transfer

ΔH_s = Sensible Enthalpy change in going from T_{ref} (298 K) to T

ΔH_R^o = Enthalpy of Reaction at standard conditions

3.2 Combustion Side Heat Transfer

The flame and combustion gases inside the chamber transfer energy into the nozzle. In order to model this interaction several assumptions had to be made. The accuracy of these assumptons must be checked during experimentation.

Assumptions

1. The combustion is at steady state conditions
2. The aluminum-water combustion reaction can be modeled as a simple fluid with properties given by NASA's Chemical Equilibrium Analysis code (CEA)
3. The nozzle can be modeled by a pipe with a diameter equal to the average of the nozzle (2 inches)
4. The flame and wall are ideal black bodies
5. The combustion particle cloud does not affect radiation
6. The nozzle is isothermal
7. Axisymmetric flow

The modes of heat transfer inside the combustor are convection and radiation. Convection can be determined by applying transport properties to the combustion mixture. This is a very complicated system so CEA is used in order to estimate the transport properties. The combustion mixture can then be assumed to be a fluid and a normal convective analysis can be used.

The Reynolds number of the system can be found using Eq 11. The accompanying Nusselt number can be found in Eq 12. The restrictions on the Nusselt number limit its accuracy in short pipes because the flow needs to be fully developed. Because the combustion flow starts father up from the nozzle it is assumed that the condition, $L/D \geq 10$, is met and the flow is fully

developed. The definition of the Nusselt number gives the convective heat transfer coefficient (Eq 13) which can be used to estimate the convection heat transfer in Eq 14.

$$Re_D = \frac{\rho u D}{\mu} = \frac{4\dot{m}}{\pi \mu D} \tag{11}$$

$$Nu_D = 0.023 Re_D^{0.8} Pr^n \tag{12}$$

Restrictions

n = 0.4 for $T_w > T_\infty$

n = 0.3 for $T_w < T_\infty$

$0.6 \leq Pr \leq 10{,}000$

$Re_D \geq 10{,}000$

$(L/D) \geq 10$

$$h = \frac{Nu_D k}{D} \tag{13}$$

$$q_{conv} = h A_{s,n} (T_\infty - T_w) \tag{14}$$

Radiation can be a large factor in heat transfer. The chamber temperature according to the CEA output. Blackbody radiation is proportional to the temperature to the fourth power as can be seen in Eq 15.

$$q_{rad} = \sigma_B A_{s,n} (T_\infty^4 - T_w^4) \tag{15}$$

3.3 Regenerative Cooling Side Heat Transfer and Pressure Drop

The cooling power of the nozzle comes from the regenerative propellant. The propellant flows in a channel within the nozzle absorbing thermal energy through convection. The propellant, oxidizer water, begins to boil. The complexity of modeling the two-phase system increases severely so several assumption must be made.

Assumptions

1. The system is at steady state
2. There is uniform heat flux into the fluid from the nozzle
3. The channel is a single horizontal tube
4. Inlet fluid is saturated liquid water
5. Outlet fluid is saturated vapor water
6. Homogenous flow
7. Constant cross sectional area

A simple diagram of the stratified horizontal two-phase flow is found in Figure 10. A simple energy balance determines that the quality of the water changes along the length, z, for a given mass flux, channel diameter, and heat flux as can be seen in Eq 16. Since the requirements for this subsystem indicate that the outlet fluid will be used as the steam oxidizer, the outlet must at least be a saturated vapor (x=1). The heat flux can be estimated from the combustion and heat transfer models derived above.

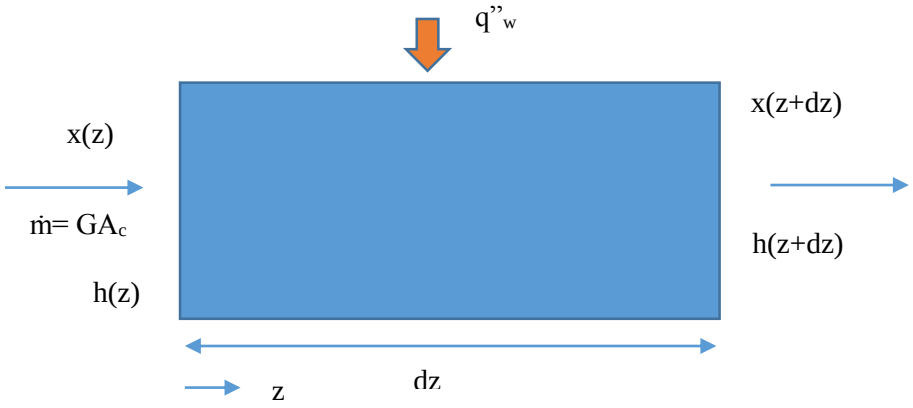

Figure 10: Energy diagram of heated flow

$$x = \frac{4q_w^{"}z}{GDh_{fg}} \tag{16}$$

The pressure drop along the channel is also of great concern. A simple model has been developed but its accuracy will need to be tested. The model assumes homogenous flow which is flow where the vapor velocity and liquid velocity are the same and the flow acts as a single combined fluid. The momentum equation (Eq 17) can be derived from Figure 11. The pressure drop across some length depends on the momentum and wall friction. Because this is a horizontal tube gravity does not have a significant effect. Properties with a bar indicate the local bulk property.

$$-\frac{dP}{dz} = \frac{d(\bar{\rho}\,\bar{u}^2)}{dz} + \left(\frac{-dP}{dz}\right)_f \tag{17}$$

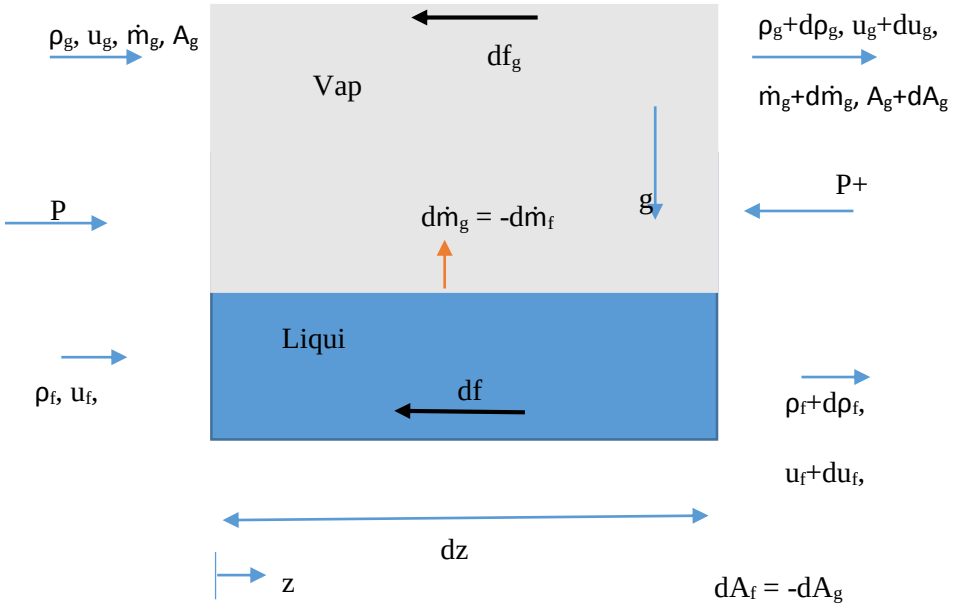

Figure 11: Two-phase flow momentum diagram

The wall friction term can be simplified using the Darcy-Weisbach equation to

$$(\frac{-dP}{dz})_f = 2f_{2\emptyset}G\bar{u}/D \tag{18}$$

Substituting Eq 18 into Eq 17 and rearranging the terms gives

$$-\frac{dP}{dz} = \frac{1}{1 + G^2x(dv_g/dp)}\left\{G^2v_{fg}\frac{dx}{dz} + 2f_{2\emptyset}G^2(v_f + xv_{fg})/D\right\} \tag{19}$$

Using the chain rule and assuming

$$G^2x(dv_g/dP) \ll 1$$

and simplifying the friction factor to

$$f_{2\emptyset} = 0.079 Re_f^{-0.25} \tag{20}$$

allows a simpler pressure drop equation to be developed in terms of the quality, x. This limits the applicability of the model to when the quality value is valid ($0 \leq x \leq 1$).

$$-\frac{dP}{dx} = G^2 v_{fg} + \frac{2 f_{2\emptyset} G^2}{D}\left(v_f + x v_{fg}\right)\frac{dz}{dx} \tag{21}$$

Integrating from x = 0 to x gives

$$-\Delta P = G^2 v_{fg} x + \frac{f_{2\emptyset} G^3 h_{fg}}{2 q_w^{"}}\left(v_f x + \frac{v_{fg} x^2}{2}\right) \tag{22}$$

Chapter 4

Conclusion

4.1 Summary of completed work

During the completion of this thesis, a rudimentary design for a regenerative nozzle and the accompanying model equations were created. The design featured an additive manufactured part that will connect to the current hardware and be able to take temperature measurements inside the combustion chamber. The cooling mechanisms of the combustor are curtain and regenerative cooling. The regenerative cooling nozzle features a single channel using oxidant water as the coolant before being injected into the combustor.

A basic model for the combustion process was developed in order to determine the parameters needed for the regenerative cooling. The parameters included potential energy produced and necessary oxidant water mass flow. A heat transfer model was also created in order to predict the energy transfer into the nozzle from the combustor side. At steady state conditions the conservation of energy dictates that the energy into the nozzle must escape through the regenerative coolant. The pressure drop across the channel was modeled assuming homogenous flow.

4.2 Recommendations for future work

The next step for this project is to build and test the nozzle design. This will allow many of the assumptions made throughout this thesis to be validated. Once the conditions are understood the nozzle design and model can be tweaked in order to increase effectiveness. For

example the design of the nozzle had a single pass channel positioned one diameter away from the wall of the inner nozzle. The actual nozzle conditions may allow for closer spacing and more effective heat transfer. Likewise the pitch of the channel is intentionally larger than necessary.

A critical consideration for future designs is the effect of startup. The initial temperature rise can cause significant thermal stresses and cause the nozzle to fail prematurely. An analysis is needed to determine the integrity of the nozzle during startup.

Other future work includes analyzing the conduction through the nozzle. Copper has several times the conductivity of Inconel and can greatly aid the heat transfer power of the nozzle if it can be incorporated.

Appendix A

Simplified Nozzle Design Drawing

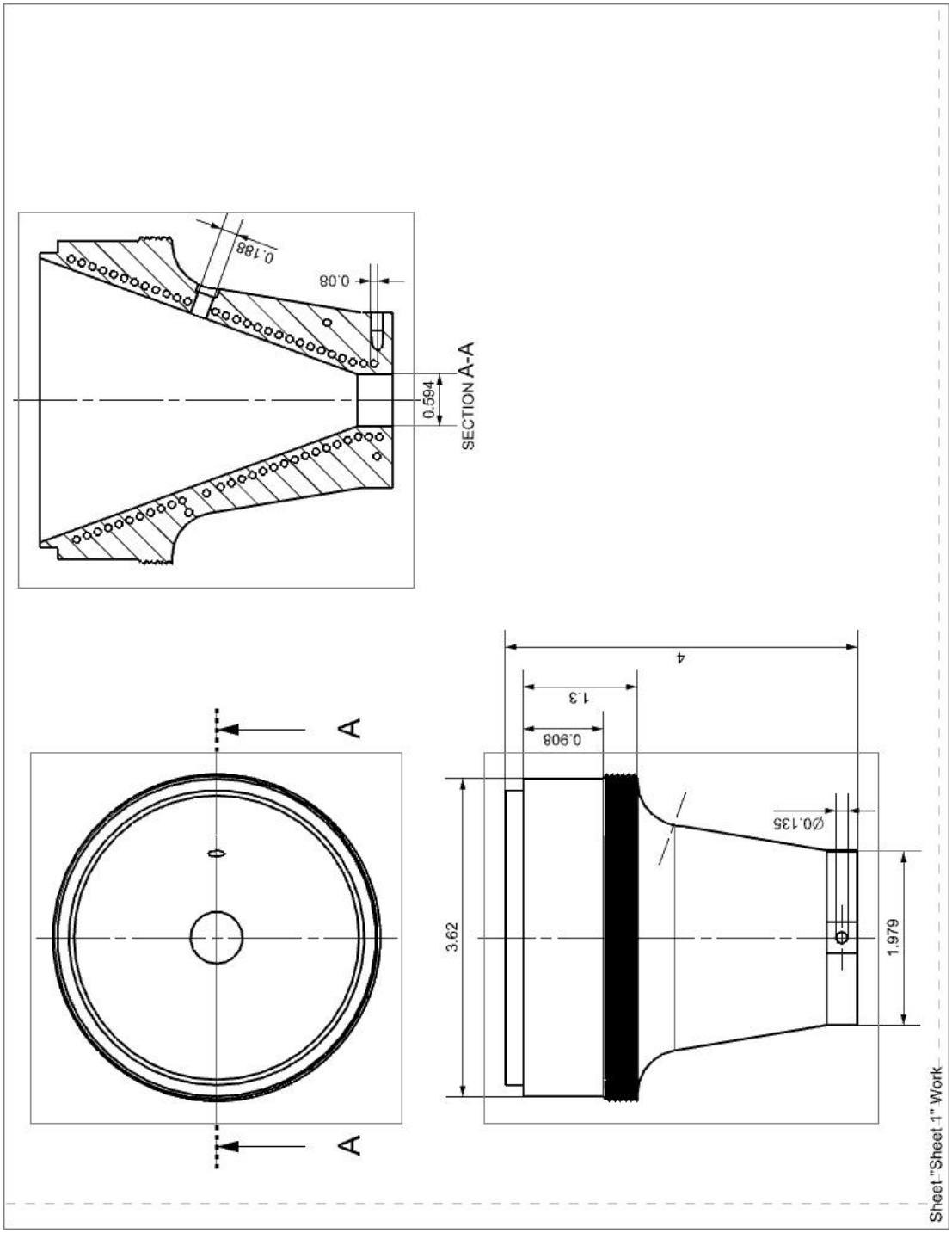

Appendix B

Sample Model Calculations

The models derived in Chapter 3 work for a wide range of conditions. A sample can be calculated by the conditions found in tables 2 and 3. The combustion heat transfer can be found by using Eq 10. The chamber pressure is assumed to be 150 psia but real conditions will need to be observed. The sensible energy of the initial components consists of only the contribution of the water vapor because it is not at standard state. The sensible energy can be found by Eq 23. Because the pressure constant heat capacity is dependent on temperature so an intermediate value will be used.

$$\Delta H_s = \dot{m} C_p \Delta T \tag{23}$$

The enthalpy of reaction is dependent on the enthalpies of formations of the products and reactants. Pressure affects the values used but its effect has been neglected. The enthalpy value used is -9257.5 KJ/kg alumina. The sensible enthalpies of the products is similar to the reactant except that the vaporization of the diluent water must be included. The total heat transfer is 0.92 kW.

ΔH_s reactants(kW)	0.42
ΔH reaction(kW)	7.93
ΔH_s products(kW)	-7.43
q_w (kW)	0.92

The heat transfer into the wall occurs as described in section 3.2. NASA's CEA program was used to determine estimates for the combustion products' properties and can be found in Appendix C. A chamber velocity of 10 m/s is assumed. This value will need to be verified in future testing but several sources [29, 30] have given values of about this magnitude. Using equations 11-15, the heat transfer was found to be 3.34 kW from convection and 3.53 kW from radiation.

The heat transfer into the regenerative coolant is through convection. The uniform heat flux was determined by dividing the heat transfer from Eq 10 by the channel surface area. Assuming the coolant entered as a saturated liquid at a pressure of 400 psia and exits as a saturated vapor, the pressure drop developed in Section 3.3 can be applied. The pressure drop across the channel is calculated to be 7 psi. Several key regenerative parameters are included here. It is also important to note that the regenerative coolant water flow rate is approximately equal to the combustion model's steam input a required by the design needs.

mass flow (g/s)	0.504
G (kg/m^2s)	155.4
Diameter(mm)	2.032
Surface area(mm^2)	29,516
Heat flux (kW/m^2)	31.01
velocity(liquid)(m/s)	0.188
max velocity(fully steam)(m/s)	11.27

From the sample calculations above it can be concluded that the combustion system and heat transfer model estimate the same magnitude of power to the nozzle. The comparable results give hope for the accuracy of this analysis.

Appendix C

CEA Code

```
        NASA-GLENN CHEMICAL EQUILIBRIUM PROGRAM CEA2, FEBRUARY 5, 2004
                  BY  BONNIE MCBRIDE AND SANFORD GORDON
       REFS: NASA RP-1311, PART I, 1994 AND NASA RP-1311, PART II, 1996

*******************************************************************************
**


 prob case=abcd9200 ro equilibrium


  ! iac problem
 o/f 4.15
 p,psia  150
 supar 1
 reac
  fuel  AL(L) wt%=100 t,k=950
  oxid H2O wt%=27.722 t,k=700
  oxid H2O(L) wt%=72.278 t,k=298.15
 output trans
 output trace=1e-5
 end

 OPTIONS: TP=F  HP=F  SP=F  TV=F  UV=F  SV=F  DETN=F  SHOCK=F  REFL=F  INCD=F
 RKT=T  FROZ=F  EQL=T  IONS=F  SIUNIT=T  DEBUGF=F  SHKDBG=F  DETDBG=F
TRNSPT=T

 TRACE= 1.00E-05  S/R= 0.000000E+00  H/R= 0.000000E+00  U/R= 0.000000E+00

 Pc,BAR =    10.342096

 Pc/P =

 SUBSONIC AREA RATIOS =

 SUPERSONIC AREA RATIOS =     1.0000

 NFZ=  1  Mdot/Ac= 0.000000E+00  Ac/At= 0.000000E+00

    REACTANT          WT.FRAC   (ENERGY/R),K   TEMP,K  DENSITY
        EXPLODED FORMULA
 F: AL(L)            1.000000   0.353193E+04   950.00  0.0000
          AL 1.00000
 O: H2O              0.277220  -0.273779E+05   700.00  0.0000
          H  2.00000  O  1.00000
 O: H2O(L)           0.722780  -0.343773E+05   298.15  0.0000
          H  2.00000  O  1.00000

  SPECIES BEING CONSIDERED IN THIS SYSTEM
```

```
(CONDENSED PHASE MAY HAVE NAME LISTED SEVERAL TIMES)
 LAST thermo.inp UPDATE:    9/09/04

 g12/97  *AL             tpis96  ALH             tpis96  ALH2
 tpis96  ALH3            tpis96  *ALO            tpis96  ALOH
 tpis96  ALO2            tpis96  AL(OH)2         tpis96  AL(OH)3
 tpis96  AL2             tpis96  AL2O            tpis96  AL2O2
 tpis96  AL2O3           g 6/97  *H              tpis96  HALO
 tpis96  HALO2           g 4/02  HO2             tpis78  *H2
 g 8/89  H2O             g 6/99  H2O2            g 5/97  *O
 g 4/02  *OH             tpis89  *O2            g 8/01  O3
 coda89  AL(cr)          coda89  AL(L)           tpis96  ALH3(a)
 tpis96  AL(OH)3(a)      tpis96  AL2O3(a)        tpis96  AL2O3(a)
 tpis96  AL2O3(a)        tpis96  AL2O3(L)        g11/99  H2O(cr)
 g 8/01  H2O(L)          g 8/01  H2O(L)

SPECIES WITH TRANSPORT PROPERTIES

       PURE SPECIES

 H                H2               H2O              O
 OH               O2

    BINARY INTERACTIONS

    H               H2
    H               O
    H2              H2O
    H2              O2
    H2O             O2
    O               O2

O/F =   4.150000

                      EFFECTIVE FUEL     EFFECTIVE OXIDANT        MIXTURE
ENTHALPY                  h(2)/R             h(1)/R               h0/R
(KG-MOL)(K)/KG        0.13090177E+03     -0.18005218E+04     -0.14254881E+04

KG-FORM.WT./KG            bi(2)              bi(1)               b0i
 *AL                  0.37062379E-01      0.00000000E+00      0.71965785E-02
 *H                   0.00000000E+00      0.11101687E+00      0.89460196E-01
 *O                   0.00000000E+00      0.55508435E-01      0.44730098E-01

POINT ITN      T            AL          H           O
ADD  AL2O3(a)
Pinf/Pt = 1.761376
Pinf/Pt = 1.765201

             THEORETICAL ROCKET PERFORMANCE ASSUMING EQUILIBRIUM

          COMPOSITION DURING EXPANSION FROM INFINITE AREA COMBUSTOR

Pin =   150.0 PSIA
CASE = abcd9200

            REACTANT                    WT FRACTION      ENERGY      TEMP
```

		(SEE NOTE)	KJ/KG-MOL	K
FUEL	AL(L)	1.0000000	29366.276	950.000
OXIDANT	H2O	0.2772200	-227633.971	700.000
OXIDANT	H2O(L)	0.7227800	-285830.088	298.150

O/F= 4.15000 %FUEL= 19.417476 R,EQ.RATIO= 1.241333 PHI,EQ.RATIO= 0.000000

	CHAMBER	THROAT	EXIT
Pinf/P	1.0000	1.7652	1.7652
P, BAR	10.342	5.8589	5.8589
T, K	1435.57	1313.10	1313.10
RHO, KG/CU M	1.9371 0	1.1997 0	1.1997 0
H, KJ/KG	-11852.2	-12142.6	-12142.6
U, KJ/KG	-12386.1	-12630.9	-12630.9
G, KJ/KG	-26930.4	-25934.4	-25934.4
S, KJ/(KG)(K)	10.5033	10.5033	10.5033
M, (1/n)	22.356	22.356	22.356
MW, MOL WT	20.692	20.692	20.692
(dLV/dLP)t	-1.00000	-1.00000	-1.00000
(dLV/dLT)p	1.0000	1.0000	1.0000
Cp, KJ/(KG)(K)	2.4007	2.3398	2.3398
GAMMAs	1.1833	1.1890	1.1890
SON VEL,M/SEC	794.8	762.0	762.0
MACH NUMBER	0.000	1.000	1.000

TRANSPORT PROPERTIES (GASES ONLY)
CONDUCTIVITY IN UNITS OF MILLIWATTS/(CM)(K)

VISC,MILLIPOISE	0.52588	0.48630	0.48630

WITH EQUILIBRIUM REACTIONS

Cp, KJ/(KG)(K)	3.0453	2.9607	2.9607
CONDUCTIVITY	2.2420	2.0313	2.0313
PRANDTL NUMBER	0.7143	0.7088	0.7088

WITH FROZEN REACTIONS

Cp, KJ/(KG)(K)	3.0450	2.9606	2.9606
CONDUCTIVITY	2.2413	2.0311	2.0311
PRANDTL NUMBER	0.7144	0.7088	0.7088

PERFORMANCE PARAMETERS

Ae/At	1.0000	1.0000
CSTAR, M/SEC	1131.3	1131.3
CF	0.6736	0.6736
Ivac, M/SEC	1402.9	1402.9
Isp, M/SEC	762.0	762.0

MOLE FRACTIONS

*H2	2.2336-1	2.2336-1	2.2336-1
H2O	7.0218-1	7.0218-1	7.0218-1

AL2O3(a) 7.4455-2 7.4455-2 7.4455-2

* THERMODYNAMIC PROPERTIES FITTED TO 20000.K

PRODUCTS WHICH WERE CONSIDERED BUT WHOSE MOLE FRACTIONS
WERE LESS THAN 1.000000E-05 FOR ALL ASSIGNED CONDITIONS

*AL	ALH	ALH2	ALH3	*ALO
ALOH	ALO2	AL(OH)2	AL(OH)3	AL2
AL2O	AL2O2	AL2O3	*H	HALO
HALO2	HO2	H2O2	*O	*OH
*O2	O3	AL(cr)	AL(L)	ALH3(a)
AL(OH)3(a)	AL2O3(L)	H2O(cr)	H2O(L)	

NOTE. WEIGHT FRACTION OF FUEL IN TOTAL FUELS AND OF OXIDANT IN TOTAL OXIDANTS

BIBLIOGRAPHY

1. Kulakov, Evgeny, and Allen F. Ross. “Aluminum Energy for Fuel Cells.” *Altek Fuel Group Inc*, 2007.
2. Domalski, Eugene. “Selected Values of Heats of Combustion and Heats of Formation of Organic Compounds Containing the Elements C, H, N, O, P, and S.” *Journal of Physical and Chemical Reference Data*, 1972, 221–78.
3. Dial, Scott. *English: A Plot of Selected Energy Densities (excluding Oxidizers).*, December 22, 2008. Own work Data Source: Energy density, Lithium-ion battery. https://commons.wikimedia.org/wiki/File:Energy_density.svg.
4. Merzhanov, A. G., Grigorjev Yu. M. and Gal'chenko Yu. A., "Aluminum Ignition", Combustion and Flame, Vol. 29, 1977, pp. 1-14.
5. Ermakov, V. A., Razdobreev A. A., Skorik A. I., Pozdeev V. V. and Smolyakov S. S., "Temperature of Aluminum Particles at the Time of Ignition and Combustion", Combustion, Explosion and Shock Waves, Vol. 18, No. 2, 1982, pp. pp 256-257.
6. Lokenbakh, A. K., Zaporina N. A., Knipele A. Z., Strod V. V. and Lepin L. K., "Effects of Heating Conditions on the Agglomeration of Aluminum Powder in Air", Combustion, Explosion & Shock Waves, Vol. 21, No. 1, 1985, pp. 73- 82
7. Beckstead, M. W. “A Summary of Aluminum Combustion.” DTIC Document, 2004.
8. Howell, John R., Mary K. Strite, and Harold E. Renkel. “Analysis of Heat-Transfer Effects in Rocket Nozzles Operating with Very High-Temperature Hydrogen.” DTIC Document, 1965.

Wang, Qiuwang, Feng Wu, Min Zeng, Laiqin Luo, and Jiguo Sun. “Numerical Simulation and Optimization on Heat Transfer and Fluid Flow in Cooling Channel of Liquid Rocket Engine

Thrust Chamber." *Engineering Computations* 23, no. 8 (December 2006): 907–21. doi:10.1108/02644400610707793.

9. Miranda, Alexander W., and Mohammad H. Naraghi. "Analysis of Film Cooling and Heat Transfer in Rocket Thrust Chamber and Nozzle." In *49th AIAA Aerospace Sciences Meeting, Orlando, Florida, AIAA-2011-0712*, 2011.
10. Terry, John E., and Gus J. Caras. "Transpiration and Film Cooling of Liquid Rocket Nozzles." DTIC Document, 1966.
11. Richter, G. Paul, and Timothy D. Smith. "Ablative Material Testing for Low-Pressure, Low-Cost Rocket Engines," 1995.
12. Batha, D., R., Carey, M., D., Campell, J., G., Coulbert, C., D., "Thrust Chamber Cooling Techniques for Spacecraft Engines", Marquardt Corporation, NAS-7-103, 1963.
13. Coulbert, C., D., "Selecting Cooling Techniques for Liquid Rockets for Spacecraft", Journal of Spacecraft and Rockets, Vol. 1, 2, 1964.
14. Huzel, D., K., Huang, D., H., "Modern Engineering for Design Liquid-Propellant Rocket Engines", AIAA,1992.
15. "Liquid Rocket Engine Fluid-Cooled Combustion Chambers," April 1, 1972.
16. Department of Mechanical Engineering. "Heat Transfer Laboratory Manual." Pennsylvania State University. n,d.
17. Buongiorno, Jacopo. "MIT22_06F10_lec13.pdf." MIT Department of Nuclear Science and Engineering, n.d.
18. S.G. Kandlikar, Fundamental issues related to flow boiling in minichannels and microchannels, Exp. Thermal Fluid Sci. 26 (2002) 389–407.

19. Cornwell, K., and Kew, P. A., Boiling in Small Parallel Channels, *Proc.CECConf. on Energy Ef. ciency in Process Technology*, Athens, Greece, October 1992, Elsevier Applied Sciences, pp. 624–638.

20. Chen, J. C., A Correlation for Boiling Heat Transfer to Saturated Fluids in Convective Flow, I&EC Process Design Devel.,vol. 5, no. 3, pp. 322–329, 1966.

21. K.E. Gungor, R.H.S. Winterton, A general correlation for flow boiling in tubes and annuli, Int. J. Heat Mass Transfer 29 (1986) 351–358.

22. M.M. Shah, A new correlation for heat transfer during flow boiling through pipes, ASHRAE Trans. 82 (2) (1976) 66–86.

23. Zhang, W., T. Hibiki, and K. Mishima. "Correlation for Flow Boiling Heat Transfer in Mini-Channels." *International Journal of Heat and Mass Transfer* 47, no. 26 (December 2004): 5749–63. doi:10.1016/j.ijheatmasstransfer.2004.07.034.

24. Kew, Peter A., and Keith Cornwell. "Correlations for the Prediction of Boiling Heat Transfer in Small-Diameter Channels." *Applied Thermal Engineering* 17, no. 8–10 (August 1997): 705–15. doi:10.1016/S1359-4311(96)00071-3.

25. R.W. Lockhart, R.C. Martinelli, Proposed correlation of data for isothermal two-phase two-component flow in pipes, Chem. Eng. Prog. 45 (1) (1949) 39–48.

26. Z. Liu, R.H.S. Winterton, A general correlation for saturated and subcooled flow boiling in tube and annuli, Int. J. Heat Mass Transfer 34 (1991) 2759–2766.

27. S.G. Kandlikar, A general correlation for saturated twophase flow boiling heat transfer inside horizontal and vertical tubes, ASME J. Heat Transfer 112 (1990) 219–228.

28. Kandlikar, S. G. “An Improved Correlation for Predicting Two-Phase Flow Boiling Heat Transfer Coefficient in Horizontal and Vertical Tubes.” *HTD (Publ.) (Am. Soc. Mech. Eng.); (United States)* HTD-VOL-27 (July 1, 1983).
29. Conrad, E. W., H. C. Parish, and J. P. Wanhainen. “Effect of Propellant Injection Velocity on Screech in 20,000-Pound Hydrogen-Oxygen Rocket Engine,” 1966.
30. Srinivasan, D. R., V. Pandurangadu, and AVSSKS Gupta. “Influence of Liquid Fuel Injection Velocities on Combustion in a Taper Can Gas Turbine Combustion Chamber.” Accessed April 3, 2016.

ACADEMIC VITA

Kevin Ciasullo
292 Midfield Drive
Ambler, PA 19002
kyc5276@psu.edu

Education

Pennsylvania State University- University Park, PA
Schreyer Honors College
Bachelor of Science in Mechanical Engineering
Minor in Engineering Entrepreneurship

Honors and Awards

Dean's List
Tau Beta Pi Honor Society

Professional Experience

Applied Research Laboratory, University Park, PA
Distinguished Undergraduate Researcher
May 2014-Present

- Working in a team to model and operate aluminum-water combustion in a power plant and a rocket
- Lead designer of a 3D printed regenerative rocket nozzle
- Worked on disassembling, assembling, and running an algae fueled turbine jet engine
- Hands on experience with machining, welding, and overall fabrication of components